Instabilities of infinite matter with effective Skyrme-type interactions

J. Margueron
GANIL, CEA/DSM-CNRS/IN2P3 Boîte Postale 5027, F-14076 Caen Cedex 05, France

J. Navarro
IFIC (CSIC-Universidad de Valencia), Apartado Postal 22085, E-46.071 Valencia, Spain

Nguyen Van Giai
Institut de Physique Nucléaire, Université Paris Sud, F-91406 Orsay Cedex, France
(Received 10 April 2002; published 3 July 2002)

The stability of the equation of state predicted by Skyrme-type interactions is examined. We consider simultaneously symmetric nuclear matter and pure neutron matter. The stability is defined by the inequalities that the Landau parameters must satisfy simultaneously. A systematic study is carried out to define interaction parameter domains where the inequalities are fulfilled. It is found that there is always a critical density ρ_{cr} beyond which the system becomes unstable. The results indicate in which parameter regions one can find effective forces to describe correctly finite nuclei and give at the same time a stable equation of state up to densities of 3–4 times the saturation density of symmetric nuclear matter.

DOI: 10.1103/PhysRevC.66.014303 PACS number(s): 21.30.Fe, 21.60.Jz, 21.65.+f, 26.60.+c

I. INTRODUCTION

Nucleon-nucleon effective interactions with an explicit density dependence have been largely employed since the seventies for studies of nuclear properties. Once the form of the interaction is chosen, either a zero-range force of Skyrme-type [1] or a finite-range force of Gogny-type [2], the parameters are determined by fitting some selected properties of doubly magic nuclei and symmetric nuclear matter at saturation. Within a Hartree-Fock (HF) scheme these interactions are able to describe quantitatively the properties of stable as well as unstable exotic nuclei. The interactions are thus well controlled around the saturation density ρ_0 of symmetric nuclear matter, for moderate isospin asymmetries and zero temperature. This type of effective interactions has also been employed to study nuclear matter in conditions of astrophysical interest, for instance, neutron matter with a finite proton fraction at densities up to several times ρ_0 and finite temperatures. This system at such conditions is relevant for studying protoneutron stars. The effective interactions are thus extrapolated to conditions of density and isospin asymmetry that are not experimentally accessible, and one should then ask for the limits of validity of such an extrapolation.

Of course, the description of nuclear matter consisting of nucleons is no longer valid beyond some value of the density, as other degrees of freedom appear. For instance, strange matter is expected beyond $(3-4)\rho_0$ [3]. For the present discussion, we shall arbitrarily accept that for densities up to $4\rho_0$, only nucleons are needed to describe nuclear matter. Even in this range of densities the effective interactions are not well determined. For instance, different effective interactions can give similar equations of state for symmetric nuclear matter and very different results for pure neutron matter. Indeed, the extreme asymmetry of isospin is not part of the usual input to determine the interaction parameters. In some cases, the determination of the parameters includes a fit to the equation of state of neutron matter calculated with microscopic methods and realistic interactions. The Skyrme interaction RATP (Rayet, Arnould, Tondeur, and Paulus) [4] takes into account the variational microscopic results of Ref. [5]. More recently, the set of SLy interactions [6,7] have included the variational results of Ref. [8] among the conditions required to fix the parameters. It is worth noting that these microscopic variational calculations are not exempt from uncertainties since realistic interactions are not completely known, especially their three-body part. Indeed, the same theoretical model [8] employing different realistic interactions leads to different equations of state, both in symmetric nuclear matter and in pure neutron matter, and sizeable differences appear for densities beyond the saturation value ρ_0. Although this type of approach gives a precious guide for the determination of the effective interaction parameters, it cannot replace the empirical data that are the natural input for the phenomenological interactions.

The extrapolation of effective interactions can result in an unphysical behavior of nuclear matter [9]. For instance, most Skyrme parametrizations predict that the isospin asymmetry energy ϵ_I becomes negative when the density is increased. Consequently, the symmetric system would be unstable at some density beyond the saturation one, preferring a largely asymmetric system made by an excess of either protons or neutrons. Another type of instability refers to the magnetic properties of neutron matter. The possibility of a ferromagnetic transition at high densities has been studied long ago, employing different theoretical ingredients, and the results were contradictory. Currently used Skyrme interactions predict that neutron matter becomes spin polarized at densities in the range $(1.1-3.5)\rho_0$ [9,10]. This transition would have important consequences for the evolution of a protoneutron star since the mean free path of neutrinos would be zero [9,11]. However, Gogny-type effective interactions either exclude such a ferromagnetic transition or predict it at very high densities [9]. Relativistic mean-field calculations [12–14] predict that such a transition could appear at densities

beyond $\simeq 4\rho_0$. Finally, recent Monte Carlo simulations [15] as well as Brueckner-Hartree-Fock calculations [16,17] using modern two- and three-body realistic interactions do exclude such an instability.

The purpose of this work is to analyze whether the presence of instabilities is inherent or not to the Skyrme-type interactions. In Sec. II we explain the restrictions on the Skyrme parameters imposed by the requirement that no instabilities should appear at densities in the range $(1-4)\rho_0$. Furthermore, the sound velocity v_s/c in matter must remain smaller than unity, and this adds a new constraint. Section III contains the discussion of the results. Conclusions are drawn in Sec. IV. Useful expressions are given in Appendixes A and B.

II. CONSTRAINTS FROM THE LANDAU PARAMETERS

The condition that the spin-unpolarized neutron matter should be the most stable phase at any density was used in Ref. [18] to constrain the Skyrme parameters. As the potential energy of the fully spin-polarized phase only depends on the combination $t_2(1+x_2)$, ferromagnetic collapse is necessarily avoided if this combination is positive. Taking into account current Skyrme parametrizations, the authors of Ref. [18] concluded that $-5/4<x_2<-1$. However, this condition is not sufficient: the family of SLy parametrizations [6,7] imposes this constraint but at densities of about 0.37 fm^{-3}, a ferromagnetism instability is predicted in neutron matter [9].

Here, we make a systematic use of the stability criteria related to the adimensional Landau parameters F_l, G_l, F_l', and G_l' in symmetric nuclear matter, and $F_l^{(n)}$ and $G_l^{(n)}$ in neutron matter. These criteria simply establish that any parameter of multipolarity l should be greater than $-(2l+1)$. Current effective interactions satisfy these conditions at saturation, and we shall investigate if they can be maintained for densities up to $4\rho_0$.

Since the original work of Skyrme and the first parametrizations for nuclear structure calculations [1], most Skyrme-like effective interactions have been built according to the following general analytical form:

$$\begin{aligned} V(\mathbf{r}_1,\mathbf{r}_2) = {} & t_0(1+x_0P^\sigma)\delta(\mathbf{r}) + \frac{1}{2}t_1(1+x_1P^\sigma)(\mathbf{k}'^2\delta(\mathbf{r}) \\ & + \delta(\mathbf{r})\mathbf{k}^2) + t_2(1+x_2P^\sigma)\mathbf{k}'\cdot\delta(\mathbf{r})\mathbf{k} \\ & + \frac{1}{6}t_3(1+x_3P^\sigma)[\rho(\mathbf{R})]^\sigma\delta(\mathbf{r}) \\ & + iW_0(\sigma_1+\sigma_2)\cdot[\mathbf{k}'\times\delta(\mathbf{r})\mathbf{k}] \end{aligned} \quad (1)$$

with $\mathbf{r}=\mathbf{r}_1-\mathbf{r}_2$, $\mathbf{R}=(\mathbf{r}_1+\mathbf{r}_2)/2$, and $\mathbf{k}=(\boldsymbol{\nabla}_1-\boldsymbol{\nabla}_2)/2i$ is the relative momentum acting on the right, and $\mathbf{k}'$ is its conjugate acting on the left. $P^\alpha=(1+\sigma_1\sigma_2)/2$ stands for the spin-exchange operator. This standard form of the Skyrme interaction contains ten parameters, eight of them denoted as t_i, x_i (with $i=0, 1, 2, 3$), the other two being the power σ of the density dependence and the strength W_0 of the zero-range spin-orbit term. These parameters are usually determined by fitting some selected properties of finite nuclei and symmetric nuclear matter. In this study we follow a different procedure, using some accepted nuclear matter values to fix as many interaction parameters as possible and using the stability criteria to put bounds on the remaining parameters.

Our starting point is given by the empirical values of the following quantities in symmetric nuclear matter at the saturation point: density ρ_0, energy per particle ϵ_0, effective mass m_0^*, compression modulus K_0, surface energy ϵ_S, and isospin asymmetry energy ϵ_I. Imposing that a Skyrme-type interaction reproduces the values of ρ_0, ϵ_0, m_0^*, and K_0 completely determines the parameters t_0, t_3, σ, and the combination $T_0\equiv[3t_1+(5+4x_2)t_2]/8$. The explicit expressions are given in Appendix A. With a Skyrme interaction, the surface energy ϵ_S depends on the previously fixed parameters, on the combination $T_S\equiv[9t_1-(5+4x_2)t_2]/8$ and on the strength W_0 of the spin-orbit term [19]. The value of W_0 is usually determined by fitting the spin-orbit splitting of some selected levels in finite nuclei, and for the present discussion we shall assume the often used value $W_0=120$ MeV fm^5. Furthermore, the symmetry energy ϵ_I can be expressed in terms of the above parameters and of the four combinations t_ix_i $(i=0-3)$. In summary, from the ten Skyrme parameters, one is kept fixed (W_0), six parameters or combinations are determined by the six empirical inputs, and three combinations are free. We found it convenient to choose the free combinations $x\equiv t_1x_1$, $y\equiv t_2x_2$, and $z\equiv t_3x_3$.

From here on, our task is to analyze the possible domains of the (x, y, z) space for different densities. For a given value of the density ρ we would like to know what is the (x, y, z) domain where no instability can occur. Stability implies that any adimensional Landau parameter of multipolarity l must be larger that $-(2l+1)$. Skyrme forces only contain monopolar and dipolar contributions to the particle-hole interaction so that all Landau parameters are zero for $l>1$. Thus, we have twelve inequalities, eight coming from symmetric nuclear matter, and four from neutron matter. Explicit expressions of the 12 Landau parameters are given in Appendix B.

Two of the twelve inequalities, however, play a special role. The condition $F_1>-3$ is trivially satisfied for any density as long as $0<m^*(\rho_0)<m$, which is the case. The Landau parameter F_0 only depends on t_1, t_3, σ, and the combination T_0, which are determined by the initial inputs. Exploring the inequality $F_0>-1$ as a function of the density, it is found that it is violated at a density smaller than ρ_0. It corresponds to a density where the compression modulus becomes negative, which is the spinodal point, i.e., the occurrence of a liquid-gas transition. Note that within a Skyrme interaction framework, the spinodal density is completely determined by the saturation properties ϵ_0, ρ_0, K_0, and m_0^*. After excluding the inequalities related to F_1 and F_0, we are left with ten inequalities to be satisfied by the yet free combinations x, y, z.

A. Symmetric nuclear matter

The parameters G_0' and G_1' give two constraints for y

$$y<-\frac{10C_1(\rho)}{3\alpha_1\rho^{2/3}}+\frac{2}{3}(T_0-2T_S), \quad (2)$$

$$y > -\frac{10C_0(\rho)}{\rho} + \frac{2}{3}(T_0 - 2T_S), \tag{3}$$

where the C_i and α_i are defined in Appendix A. The parameters F_1', G_1 give two constraints on combinations of x and y:

$$x - \frac{3}{5}y > -\frac{4C_0(\rho)}{\rho} + \frac{4}{15}(T_0 - 2T_S), \tag{4}$$

$$x + \frac{3}{5}y < \frac{4C_0(\rho)}{\rho} - \frac{4}{15}(T_0 - 2T_S). \tag{5}$$

The remaining Landau parameters G_0 and F_0' constrain combinations of all three x, y, and z unknowns:

$$\frac{1}{9\alpha_1}(\rho^\sigma - \rho_0^\sigma)z + (\rho^{2/3} - \rho_0^{2/3})x + \frac{3}{5}(\rho^{2/3} + \rho_0^{2/3})y > \frac{4}{3\alpha_1}\left(C_1(\rho) + C_1(\rho_0) + \frac{2\epsilon_I}{\rho_0}\right) - \frac{4}{15}(\rho^{2/3} + \rho_0^{2/3})(T_0 - 2T_S), \tag{6}$$

$$-\frac{1}{9\alpha_1}(\rho^\sigma - \rho_0^\sigma)z - (\rho^{2/3} - \rho_0^{2/3})x + \frac{3}{5}(\rho^{2/3} - \rho_0^{2/3})y > \frac{4}{3\alpha_1}\left(C_1(\rho) - C_1(\rho_0) - \frac{2\epsilon_I}{\rho_0}\right) - \frac{4}{15}(\rho^{2/3} - \rho_0^{2/3})(T_0 - 2T_S). \tag{7}$$

However, it is possible to take the linear combination $F_0' + G_0$ to get another constraint independent of z. Note that Eq. (7) reduces to the trivial condition $\epsilon_I > 0$ when $\rho = \rho_0$. It is due to the fact that the symmetry energy ϵ_I has been used to write x_0 in terms of the remaining parameters.

B. Neutron matter

The parameters $F_1^{(n)}$, and $G_1^{(n)}$ give two constraints on combinations of x and y:

$$x - \frac{3}{5}y < \frac{4C_0(\rho)}{\rho} + \frac{4}{15}(T_0 - 2T_S), \tag{8}$$

$$x - \frac{1}{5}y < \frac{2C_0(\rho)}{\rho} - \frac{2}{15}(T_0 - 2T_S). \tag{9}$$

The remaining Landau parameters $F_0^{(n)}$, and $G_0^{(n)}$ constrain combinations of all three x, y, z parameters:

$$\frac{(\sigma+1)(\sigma+2)\rho^\sigma - 2\rho_0^\sigma}{6(4\alpha_2\rho^{2/3} - 3\alpha_1\rho_0^{2/3})}z + x - \frac{3}{5}y < \frac{4}{4\alpha_2\rho^{2/3} - 3\alpha_1\rho_0^{2/3}}\left(C_1(\rho_0) - C_2(\rho) + \frac{2\epsilon_I}{\rho_0}\right) + \frac{4}{15}(T_0 - 2T_S), \tag{10}$$

$$\frac{1}{9}(\rho^\sigma - \rho_0^\sigma)z + \frac{1}{3}(2\alpha_2\rho^{2/3} - 3\alpha_1\rho_0^{2/3})x + \frac{1}{5}(2\alpha_2\rho^{2/3} + 3\alpha_1\rho_0^{2/3})y > \frac{4}{3}\left(C_1(\rho_0) + C_3(\rho) + \frac{2\epsilon_I}{\rho_0}\right) - \frac{4}{45}(7\alpha_2\rho^{2/3} + 3\alpha_1\rho_0^{2/3})(T_0 - 2T_S). \tag{11}$$

Note that the linear combination $\alpha_1 F_0' + G_0^{(n)}$ gives another constraint independent of z.

C. Sound velocity constraint

In addition to the constraints from stability requirements it is important to check that for each density the sound velocity v_s remains smaller than the speed of light, i.e., superluminosity does not occur. The sound velocity is directly related to the compression modulus $K(\rho)$ that can itself be expressed in terms of the Landau parameters F_0 and F_1:

$$m v_s^2 = \frac{1}{9}K = \frac{\hbar^2 k_F^2}{3m}\frac{1 + F_0}{1 + \frac{1}{3}F_1}. \tag{12}$$

In symmetric nuclear matter it turns out that v_s depends only on the parameters t_0, t_3, σ, and the combination T_0, all of which being already determined by the six initial empirical inputs. Therefore, there will be no additional bounds on the allowed volume in (x, y, z) space. However, Eq. (12) shows that v_s increases with increasing density and for a given choice of initial empirical inputs there is always a value ρ_{sound} beyond which v_s/c is greater than 1. The value of ρ_{sound} depends essentially on the adopted value for K_0. For instance, ρ_{sound} is around $3.5\rho_0$ if $K_0 = 350$ MeV and it may become $6\rho_0$ if $K_0 = 250$ MeV. Thus, there is no Skyrme interaction that can be reasonably be used beyond ρ_{sound} because it would predict unphysical values of the sound velocity.

The situation is somewhat different in pure neutron matter. Now, the Landau parameters in Eq. (12) depend also on the (x, y, z) parameter combinations. The requirement that v_s/c remains smaller than unity adds one more constraint to the determination of the allowed volume in the (x, y, z) space. We shall see in the following section that the sound velocity in neutron matter does not bring any effective re-

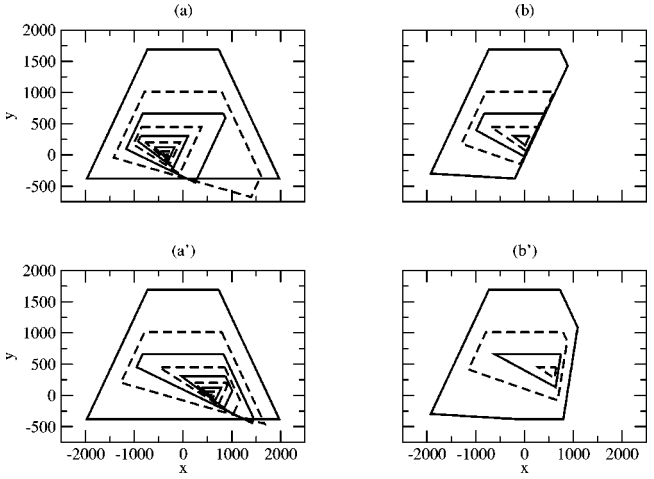

FIG. 1. Comparison of the sections of the volume $\Omega(\rho)$ by a horizontal plane $z=$const, in units of MeV fm$^{3(1+\sigma)}$. The horizontal and vertical axes are for the parameters x and y, respectively, in units of MeV fm^5. Cases (a) and (a′) correspond to the constraints from the Landau parameters of symmetric nuclear matter. Cases (b) and (b′) include also the constraints from neutron matter. Two values of z have been used, namely, $z=2\times10^4$ for cases (a) and (b), and $z=-2\times10^4$ for cases (a′) and (b′). The different closed contours correspond to different values of ρ. The largest area is for $\rho=\rho_0$, the next one corresponds to an increase by a step of $0.5\rho_0$, and so on. For the sake of clarity, they are alternatively represented by solid and dashed lines.

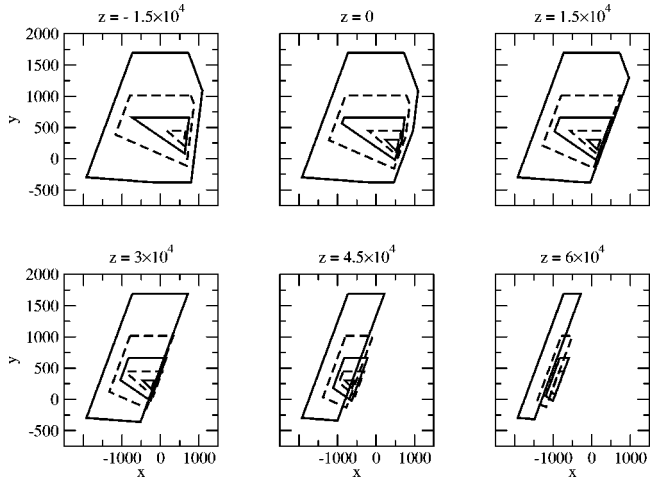

FIG. 2. Comparison of the sections of the volume $\Omega(\rho)$ by a horizontal plane, for choices of z different from Fig. 1. The various closed contours correspond to different values of ρ. The largest area is for $\rho=\rho_0$, the next one corresponds to an increase by a step of $0.5\rho_0$, and so on. The calculations are done using the full constraints. The values of z are in units of MeV fm$^{3(1+\sigma)}$.

striction on the allowed volume in the parameter space, at least around the values of the six empirical inputs used in the present study.

We must mention that a study of the sound velocity in asymmetric nuclear matter was made in Ref. [20]. The aim was to find the conditions to be satisfied by the Skyrme parameters so that superluminosity would never appear at any density whatsoever. The conditions that were found are very restrictive. In the present work, our point of view is quite different since we do not think that the Skyrme effective approach should be valid at densities beyond $4\rho_0$.

III. RESULTS AND DISCUSSION

The inputs used in the present study are $\epsilon_0=-16.0$ MeV, $\rho_0=0.16$ fm^{-3}, $K_0=230$ MeV, $m_0^*/m=0.70$, $\epsilon_S=18.0$ MeV, and $\epsilon_I=32.0$ MeV.

For a given value of the density ρ, the various constraints define in the (x, y, z) parameter space an allowed volume that we call Ω. The surface of $\Omega(\rho)$ is made of planes because all constraints are linear in x, y, z. Any point outside Ω is forbidden because some of the inequalities would not be fulfilled. To present the results and facilitate the discussion we will explore the z axis. The intersection of a volume $\Omega(\rho)$ with a $z=$const horizontal plane gives a polygon that can be represented in the (x, y) plane. By varying ρ in the range $\rho_0-4\rho_0$ one can follow the evolution of the polygons. The vanishing of the area of the polygon at some critical density $\rho_{\rm cr}$ indicates that there is no Skyrme interaction (having the chosen value of z) which can fulfill the chosen set of constraints at densities beyond $\rho_{\rm cr}$.

We have performed two types of calculations: (a) using only the six constraints from the Landau parameters of symmetric nuclear matter and disregarding those of neutron matter; (b) using all eleven constraints from symmetric nuclear matter and neutron matter plus the sound velocity constraint in neutron matter. In Fig. 1 are displayed some typical results. We have chosen a positive and a negative value of z since there is no *a priori* limitation on z. The value $z=2\times10^4$ MeV fm$^{3(1+\sigma)}$ correspond to Figs. 1(a) and 1(b), and $z=-2\times10^4$ to Figs. 1(a′) and 1(b′). Results involving only Landau parameters of symmetric matter are displayed in Figs. 1(a) and 1(a′), whereas Figs. 1(b) and 1(b′) correspond to results using all eleven constraints. The contours are drawn every $0.5\rho_0$ starting from ρ_0.

Let us first examine the results without neutron matter constraints [Figs. 1(a) and 1(a′)]. At $\rho=\rho_0$ the contour is a polygon whose upper and lower horizontal sides are determined by the constraints on G_0' and G_0, respectively, whereas the left and right sides correspond to F_1' and G_1. When ρ increases the lower side becomes tilted and the constraint on F_0' gradually appears as a new side on the right hand side of the polygon. At $\rho\simeq2\rho_0$ and above the F_0' constraint is dominating over the G_1 constraint. The surface of the polygon shrinks as ρ increases. The value of $\rho_{\rm cr}$ is above $4.5\rho_0$. This value is reached for x and y both negative if z is positive, whereas for z negative $\rho_{\rm cr}$ corresponds to $x\geqslant0$ and $y\leqslant0$.

The situation changes somewhat when neutron matter constraints are added [Figs. 1(b) and 1(b′)]. At $\rho=\rho_0$ the lower side is given by the $G_0^{(n)}$ constraint while the right side of the polygon is mainly determined by the $F_0^{(n)}$ constraint that limits severely the allowed area. It must be noted that the sound velocity does not bring any limitation on the $(x, y,$

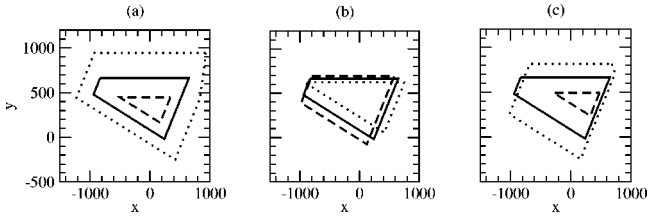

FIG. 3. Sensitivity to some empirical inputs. Case (a) results for $m_0^*/m=0.6$, 0.7, and 0.8 (respectively, dotted, solid, dashed), keeping the remaining empirical inputs to their fixed values. Case (b) same as (a), with $K_0=210$, 230, and 250 MeV (respectively, dotted, solid, dashed). Case (c) same as (a), with the surface energy $\epsilon_S=16$, 18, and 20 MeV (respectively, dotted, solid, dashed). All cases have been calculated for $z=10^4$ MeV fm$^{3(1+\sigma)}$ and $\rho=2\rho_0$.

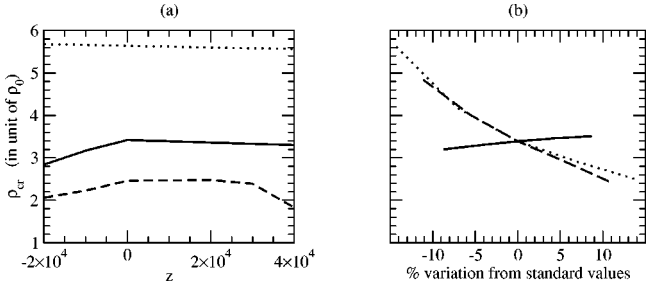

FIG. 4. Case (a) ρ_{cr} as a function of z [in units of MeV fm$^3(1+\sigma)$] for different values of $m_0^*/m=0.6$, 0.7, 0.8 (respectively, dotted, solid, dashed). Case (b) ρ_{cr} as a function of relative variations of some empirical inputs; dotted line: variation of m_0^*/m, solid line: variation of K_0, dashed line: variation of ϵ_S.

z) parameters in the domain explored here. One can see that the critical density ρ_{cr} has now a lower value as compared to the case of Figs. 1(a) and 1(a)′.

There is no natural limitation to the domain of the z parameter and therefore, we must explore the dependence of the results on z. In Fig. 2 we present calculations where all eleven constraints are included, exploring the z axis from negative to positive values. The interpretation of the different sides delimitating the contours is the same as in the case of Fig. 1. One can see that ρ_{cr} is highest when z is between 0 and 3×10^4. For negative values of z the allowed area at $\rho=2.5\rho_0$ is already fairly small. Below $z\simeq3\times10^4$ the polygons of larger ρ are contained inside those of smaller ρ, i.e., interactions stable at density ρ are also stable at all densities between ρ_0 and ρ. For z larger than 3×10^4 the allowed areas at larger ρ tend to move outside the area of $\rho=\rho_0$, which means that such interactions might seem acceptable at large densities but they have the defect of having instabilities at normal density.

So far we have discussed the results obtained with the values of empirical inputs as adopted in Sec. II. It is interesting to see how the conclusions may depend on this choice. In Fig. 3 we study, for a fixed value of $\rho=2\rho_0$ and a chosen $z=10^4$ MeV fm$^{3(1+\sigma)}$, the evolution of the allowed polygons when one changes one of the empirical inputs: the effective mass m_0^*/m [Fig. 3(a)], the incompressibility K_0 [Fig. 3(b)], the surface energy ϵ_S [Fig. 3(c)]. It can be seen that the results are sensitive to the value of m_0^*/m. A smaller value of m_0^*/m makes the allowed domain larger and therefore, the critical density ρ_{cr} is shifted to higher values. On the contrary, the allowed domain is reduced when higher values of m_0^*/m are considered, and instabilities appear for densities below $2\rho_0$. Hence, to avoid low density instabilities, one should prefer low m_0^*/m. The sensitivity to ϵ_S is also non-negligible, whereas the dependence on K_0 is moderate.

In Fig. 4 we present the calculated values of the critical density ρ_{cr} (in units of ρ_0). Figure 4(a) shows ρ_{cr} as a function of the parameter z for various choices of the empirical input m_0^*/m around the value 0.70. As pointed out above, one can see clearly that it is more favorable to choose z positive and less than 3×10^4 in order to have ρ_{cr} not too small, and that larger values of m_0^*/m tend to yield lower ρ_{cr}. The three curves of Fig. 4(b) represent ρ_{cr} as a function of the relative variations (in percentage) around the standard choice of m_0^*/m, K_0 and ϵ_S. The value of z is fixed at 10^4 MeV fm$^{3(1+\sigma)}$. These curves show that ρ_{cr} depends little on K_0 whereas moderate increases of m_0^*/m (from 0.70 to 0.75), or of ϵ_S (from 18 to 20 MeV) can lower ρ_{cr} below $3\rho_0$.

Now, the question arises whether these bounds for Skyrme parameters are useful or not for calculations in pure nucleon matter and finite nuclei. In principle, we expect a qualitative positive answer for finite nuclei because the used inputs guarantee that the first terms in a leptodermous expansion of the mass formula are well described. To be more quantitative, we have constructed several parametrizations

TABLE I. Skz$n$ parametrizations. All of them have the following common values: $\sigma=0.1694$, $t_0=-2471.10$ MeV fm^3, $t_1=439.85$ MeV fm^5, and $t_3=13\,732.8$ MeV fm$^{3(1+\sigma)}$, as they come from the initial inputs.

	z MeV fm$^{3(1+\sigma)}$	x MeV fm^5	y MeV fm^5	t_2 MeV fm^5	x_0	x_1	x_2	x_3
Skz-1	-10^4	570.42	266.2	-299.14	-0.2665	1.2968	-0.8899	-0.7282
Skz0	0	458.0	215.0	-258.18	0.1986	1.0413	-0.8328	0.0
Skz1	10^4	217.0	221.0	-262.98	0.6052	0.4933	-0.8404	0.7282
Skz2	2×10^4	24.0	227.0	-267.78	1.0290	0.0546	-0.8478	1.4564
Skz3	3×10^4	-265.5	233.1	-272.66	1.4174	-0.6082	-0.8549	2.1846
Skz4	4×10^4	-512.0	239.15	-277.50	1.8226	-1.1640	-0.8618	2.9127

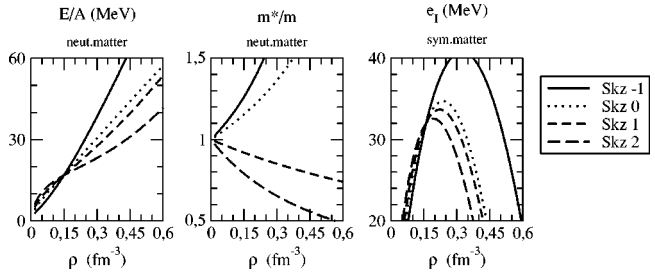

FIG. 5. Predictions of several Skz*n* parametrizations for the binding energy and the effective mass of pure neutron matter and for asymmetry energy as function of the density.

using the following criteria. We first fix an arbitrary value of z, going from -10^4 to 4×10^4, and then we take the values of x and y as the coordinates of the point $\Omega(\rho_{\rm cr})$. In this way instabilities are pushed to the highest values of the density. The sets of parameters are dubbed Skz*n* and they are given in Table I. Of course, the criteria of highest value of $\rho_{\rm cr}$ is purely arbitrary but our intention here is just to explore the resulting parametrizations and not to give the best parameter set. In Fig. 5 are displayed the results for pure neutron matter. One can see that choosing negative values of z results in an increasing neutron effective mass for increasing densities. On the other side, values of z greater than 2×10^4 produce too low binding energies. We have then restricted our calculations in finite nuclei to parametrizations Skz0, Skz1, and Skz2. In Table II are displayed the ground state binding energies and charge radii of some doubly magic nuclei together with the results obtained with SIII and SLy4 interactions. The results are reasonably satisfactory. We have noticed that convergence problems occur with Skz0 when looking for the HF solution of ^{208}Pb. To obtain better results one should relax the condition of highest value for the critical density, and of course include some finite nuclei results in the fine tuning of the parameters.

IV. CONCLUSION

In this work we have explored the parameter domains of Skyrme-type forces where the stability conditions related to Landau parameters inequalities can be satisfied up to densities of the order of $4\rho_0$. Stability of both nuclear matter and pure neutron matter are considered. We have taken advantage of the possibility to characterize the domains by analytical expressions. Starting from a general Skyrme force containing ten parameters, we have shown that seven parameters or combinations thereof can be approximately fixed by physical quantities which can be considered experimentally known to some extent. Thus, the problem reduces to the study of allowed domains in a three-dimensional space spanned by three parameter combinations.

The results show that, for any Skyrme-type interaction there is a critical density $\rho_{\rm cr}$ above which one cannot insure all stability conditions. This critical density does not exceed $(3.5-4)\rho_0$ for a reasonable choice of empirical inputs. It is nevertheless an interesting result to know that it is possible to find Skyrme-type interactions that can give stable nuclear matter and neutron matter up to such densities. The parameter domains are well identified and it would be worthwhile to look inside those domains for Skyrme interactions that can also describe accurately finite nuclei. Our exploration with parametrizations Skz*n* has shown that reasonable ground state binding energies and charge radii can be obtained. A more systematic study over a wide number of nuclei would be necessary to get the Skyrme-type interaction that is stable over the largest range of densities. This new interaction would be very useful for neutron star calculations, as for instance, the neutrino mean free path or the URCA process.

The present analysis is restricted to Skyrme interactions, because the simplicity of the resulting expressions allows for an algebraic study. The presence of instabilities in nuclear matter and neutron matter beyond some critical density could be attributed to the zero-range form of the interaction, and its k^2 dependence of the effective masses. Finite range effective interactions [2] are an alternative choice for describing the equation of state of nuclear and neutron matter. We know that the actual parametrizations (D1,D1S,D1P) do not predict instabilities [9] for densities below $\simeq 5\rho_0$. We have not considered a systematic study of Gogny effective interactions because they contain more parameters, and they do not allow for a simple algebraic analysis.

ACKNOWLEDGMENTS

We have greatly benefited from fruitful discussions with our late colleague Dominique Vautherin on this subject and we acknowledge his invaluable help. This work was partly supported by DGI (Spain), Grant No. BFM2001-0262. J.N. and N.V.G. thank GANIL for its hospitality during completion of the work.

TABLE II. HF binding energies and charge radii for several Skz*n* parametrizations. NC means that the HF calculation has not converged.

Nucleus	Observable	Skz0	Skz1	Skz2	Expt.	*S*III	SLy4
^{16}O	B/A (MeV)	8.39	8.38	8.38	7.98	7.95	7.97
	r_c (fm)	2.76	2.76	2.76	2.73	2.76	2.80
^{40}Ca	B/A (MeV)	8.87	8.85	8.85	8.55	8.48	8.55
	r_c (fm)	3.47	3.47	3.47	3.49	3.50	3.51
^{208}Pb	B/A (MeV)	NC	7.97	7.91	7.87	7.79	7.80
	r_c (fm)	NC	5.48	5.49	5.50	5.58	5.52

APPENDIX A: NUCLEAR MATTER RELATIONS

Employing a Skyrme interaction, the energy density of semi-infinite symmetric nuclear matter is written as

$$\mathcal{H}=\frac{\hbar^2}{2m^*}\tau+\frac{3}{8}t_0\rho^2+\frac{1}{16}t_3\rho^{\sigma+2}+\frac{1}{8}T_S|\nabla\rho|^2 - \frac{m^*}{\hbar^2}V_{so}\rho|\nabla\rho|^2, \tag{A1}$$

where $V_{so}=9W_0^2/16$.

Denoting by ρ_0, ϵ_0, K_0, and m_0^*, respectively, the density, energy per particle, compressibility, and effective mass at saturation of the bulk symmetric nuclear matter, it turns out that the Skyrme parameters t_0, t_3, σ, and the combination T_0 can be written as

$$T_0=\left(\frac{\hbar^2}{m_0^*}-\frac{\hbar^2}{m}\right)\frac{1}{\rho_0}, \tag{A2}$$

$$\sigma=\frac{\frac{1}{9}K_0+\epsilon_0+\left(\frac{\hbar^2}{10m}-\frac{2\hbar^2}{15m_0^*}\right)k_F^2(0)}{-\epsilon_0+\left(\frac{3\hbar^2}{10m}-\frac{\hbar^2}{5m_0^*}\right)k_F^2(0)}, \tag{A3}$$

$$t_3=\frac{16}{\rho_0^{1+\sigma}}\frac{1}{\sigma}\left[-\epsilon_0+\left(\frac{3\hbar^2}{10m}-\frac{\hbar^2}{5m_0^*}\right)k_F^2(0)\right], \tag{A4}$$

$$t_0=\frac{8}{3\rho_0}\left[\epsilon_0-\frac{3\hbar^2}{10m_0^*}k_F^2(0)-\frac{1}{16}t_3\rho_0^{1+\sigma}\right], \tag{A5}$$

where $\rho_0=2/(3\pi)^2k_F^3(0)$. Once the parameters t_0, t_3, σ, and the combination T_0 have been fixed, the surface energy only depends on the combination T_S and the spin-orbit strength W_0. The surface energy can be written as an integral over the density [19]

$$\epsilon_S=8\pi r_0^2\int_0^{\rho_0}d\rho\left[\frac{\hbar^2}{36m}-\frac{5}{36}T_0\rho+\frac{1}{8}T_S\rho-\frac{m^*}{\hbar^2}V_{so}\rho^2\right]^{1/2} \times\left[\frac{3\hbar^2}{10m^*}k_F^2+\frac{3}{8}t_0\rho+\frac{1}{16}t_3\rho^{\sigma+1}\right]^{1/2}, \tag{A6}$$

where $r_0=[3/(4\pi\rho_0)]^{1/3}$ is the unit radius, and a Thomas-Fermi approximation up to $\hbar^2$ order has been used to replace the kinetic energy density.

Then, the following relation involving the symmetry energy ϵ_I can be used to relate x_0 to the already known parameter combinations and to the free parameters (x, y, z):

$$t_0x_0=\left(-\frac{3}{2}x+\frac{9}{10}y+\frac{2}{5}(T_0-2T_S)\right)\alpha_1\rho_0^{2/3}-\frac{1}{6}z\rho_0^{\sigma} -2C_1(\rho_0)-\frac{4\epsilon_I}{\rho_0}. \tag{A7}$$

To simplify the notation used in Sec. II we have introduced the following functions of the density:

$$C_0(\rho)=\frac{\hbar^2}{m}+T_0\rho, \tag{A8}$$

$$C_1(\rho)=-\left(\frac{\hbar^2}{m}+T_0\rho\right)\frac{\alpha_1}{\rho^{1/3}}+\frac{1}{4}t_0+\frac{1}{24}t_3\rho^{\sigma}, \tag{A9}$$

$$C_2(\rho)=-\frac{1}{2}\left(\frac{\hbar^2}{m}+4T_0\rho\right)\frac{\alpha_2}{\rho^{1/3}}-\frac{1}{2}t_0 -\frac{1}{24}(\sigma+1)(\sigma+2)t_3\rho^{\sigma}, \tag{A10}$$

$$C_3(\rho)=-\frac{1}{2}\left(\frac{\hbar^2}{m}+T_0\rho\right)\frac{\alpha_2}{\rho^{1/3}}+\frac{1}{2}t_0+\frac{1}{12}t_3\rho^{\sigma}, \tag{A11}$$

which contain only known parameters. We have also introduced the constants

$$\alpha_1=\left(\frac{\pi^4}{12}\right)^{1/3},\quad \alpha_2=\left(\frac{\pi^4}{3}\right)^{1/3}. \tag{A12}$$

APPENDIX B: LANDAU PARAMETERS

The Landau parameters in symmetric nuclear matter are

$$F_0=\left(\frac{3}{4}t_0+\frac{1}{16}(\sigma+1)(\sigma+2)t_3\rho^{\sigma}\right)\frac{2m^*k_F}{\hbar^2\pi^2}-F_1, \tag{B1}$$

$$G_0=\left(\frac{1}{4}t_0(2x_0-1)+\frac{1}{24}t_3\rho^{\sigma}(2x_3-1)\right)\frac{2m^*k_F}{\hbar^2\pi^2}-G_1, \tag{B2}$$

$$F_0'=\left(-\tfrac{1}{4}t_0(2x_0+1)-\frac{1}{24}t_3\rho^{\sigma}(2x_3+1)\right)\frac{2m^*k_F}{\hbar^2\pi^2}-F_1', \tag{B3}$$

$$G_0'=\left(-\frac{1}{4}t_0-\frac{1}{24}t_3\rho^{\sigma}\right)\frac{2m^*k_F}{\hbar^2\pi^2}-G_1', \tag{B4}$$

$$F_1=-3T_0\frac{m^*}{\hbar^2}\rho, \tag{B5}$$

$$G_1=-3T_1\frac{m^*}{\hbar^2}\rho, \tag{B6}$$

$$F_1'=3T_2\frac{m^*}{\hbar^2}\rho, \tag{B7}$$

$$G_1'=3T_3\frac{m^*}{\hbar^2}\rho, \tag{B8}$$

where the T_i's are the following parameter combinations:

$$T_0=\tfrac{1}{8}[3t_1+5t_2+4y], \tag{B9}$$

$$T_1=\tfrac{1}{8}[2x+2y-t_1+t_2], \tag{B10}$$

$$T_2=\tfrac{1}{8}[2x-2y+t_1-t_2], \tag{B11}$$

$$T_3=\tfrac{1}{8}[t_1-t_2], \tag{B12}$$

and the effective mass is

$$\frac{\hbar^2}{m^*}=\frac{\hbar^2}{m}+T_0\rho. \tag{B13}$$

The Landau parameters in neutron matter are

$$F_0^{(n)}=\left(\frac{1}{2}t_0(1-x_0)+\frac{1}{24}(\sigma+1)(\sigma+2)t_3\rho^\sigma(1-x_3)\right)\times\frac{m_n^*k_F}{\hbar^2\pi^2}-F_1^{(n)}, \tag{B14}$$

$$G_0^{(n)}=\left(\frac{1}{2}t_0(x_0-1)+\frac{1}{12}t_3\rho^\sigma(x_3-1)\right)\frac{m_n^*k_F}{\hbar^2\pi^2}-G_1^{(n)}, \tag{B15}$$

$$F_1^{(n)}=-3(T_0-T_2)\frac{m_n^*}{\hbar^2}\rho, \tag{B16}$$

$$G_1^{(n)}=-3(T_1-T_3)\frac{m_n^*}{\hbar^2}\rho, \tag{B17}$$

and the effective mass is

$$\frac{\hbar^2}{m_n^*}=\frac{\hbar^2}{m}+(T_0-T_2)\rho. \tag{B18}$$

[1] D. Vautherin and D. M. Brink, Phys. Rev. C **5**, 626 (1972).
[2] D. Gogny, in *Proceedings of the International Conference on Nuclear Self-consistent Fields*, edited by G. Ripka and M. Porneuf (North-Holland, Amsterdam, 1975).
[3] M. Baldo, G. F. Burgio, and H. J. Schulze, Phys. Rev. C **61**, 055801 (2000).
[4] M. Rayet, M. Arnould, F. Tondeur, and G. Paulus, Astron. Astrophys. **116**, 183 (1982).
[5] B. Friedman and V. R. Pandharipande, Nucl. Phys. **A361**, 502 (1981).
[6] E. Chabanat, P. Bonche, P. Haensel, J. Meyer, and R. Schaeffer, Nucl. Phys. **A627**, 710 (1997).
[7] E. Chabanat, P. Bonche, P. Haensel, J. Meyer, and R. Schaeffer, Nucl. Phys. **A635**, 231 (1998).
[8] R. B. Wiringa, V. Fiks, and A. Fabrocini, Phys. Rev. C **38**, 1010 (1988).
[9] J. Margueron, Ph.D. thesis, Université Paris XI Orsay, 2001.
[10] A. Vidaurre, J. Navarro, and J. Bernabeu, Astron. Astrophys. **135**, 361 (1984).
[11] J. Navarro, E. S. Hernández, and D. Vautherin, Phys. Rev. C **60**, 045801 (1999).
[12] R. Niembro, S. Marcos, M. L. Quelle, and J. Navarro, Phys. Lett. B **249**, 373 (1990).
[13] S. Marcos, R. Niembro, M. L. Quelle, and J. Navarro, Phys. Lett. B **271**, 277 (1991).
[14] P. Bernardos, S. Marcos, R. Niembro, and M. L. Quelle, Phys. Lett. B **356**, 175 (1995).
[15] S. Fantoni, A. Sarsa, and K. E. Schmidt, Phys. Rev. Lett. **87**, 181101 (2001).
[16] I. Vidaña, A. Polls, and A. Ramos, Phys. Rev. C **65**, 035804 (2002).
[17] U. Lombardo *et al.* (private communication).
[18] M. Kutschera and W. Wójcik, Phys. Lett. B **325**, 271 (1994).
[19] J. Treiner and H. Krivine, Ann. Phys. (N.Y.) **170**, 406 (1986).
[20] R. K. Su, H. Q. Song, and T. T. S. Kuo, Phys. Rev. C **37**, 1770 (1988).